JACS
JOURNAL OF THE AMERICAN CHEMICAL SOCIETY

ARTICLE

pubs.acs.org/JACS

Controlling the Transmission of Stereochemical Information through Space in Terphenyl-Edged Fe_4L_6 Cages

Wenjing Meng,[†] Jack K. Clegg,[†] John D. Thoburn,[†,‡] and Jonathan R. Nitschke*[,†]

[†]Department of Chemistry, University of Cambridge, Lensfield Road, Cambridge CB2 1EW, U.K.

[‡]Department of Chemistry, Randolph-Macon College, Ashland, Virginia 23005, United States

Supporting Information

ABSTRACT: A series of terphenyl-edged Fe_4L_6 cages were synthesized from substituted 4,4″-diamino-*p*-terphenyls, 2-formylpyridine, and iron(II). For the parent diaminoterphenyl, all three possible diastereomers, with *T*, S_4, and C_3 point symmetries, were formed in nearly equal amounts, as determined by ^{1}H and ^{13}C NMR. When 2,2″-dimethylterphenylenediamine was used, the *T*-symmetry diastereomer was observed to predominate. The use of 2′,3′,5′,6′-tetramethylterphenylenediamine generated predominantly the S_4 cage diastereomer, whereas 2′,5′-dimethylterphenylenediamine produced the C_3-symmetric cage to a greater degree than the other two diastereomers. The factors contributing to the transfer of chiral information between metal vertices were analyzed, and the general principles underlying the delicately balanced thermodynamics were determined.

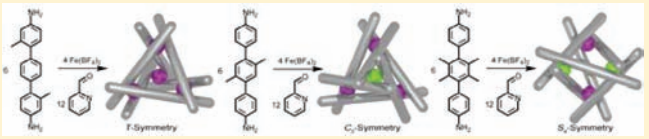

INTRODUCTION

Self-assembled polyhedral metal−organic cages[1−8] have received recent attention because of their ability to alter the chemical reactivity of other species in solution.[9−11] Recent examples include the use of cages as catalysts[12−15] or photoreactors,[16,17] the stabilization of reactive species,[18−21] and the generation of unusual reaction products.[21−24] The search for new functions has driven the exploration of new cage geometries, including boxes, prisms, cubes,[25−29] and large spherical structures reminiscent of virus capsids.[30]

The importance of being able to manipulate the stereochemistry of chiral cages is highlighted by recent applications of cages in stereoselective transformations[23] and chiral recognition,[22] which both involve tetrametallic cages with approximately tetrahedral symmetry. The great majority of M_4L_6 cages reported so far[31−36] exhibit simple chirality in solution, forming homochiral species with all four metal ions at each vertex within the cage possessing the same Λ or Δ chirality, giving the molecule *T* point symmetry.[32,35,37−42] Here we present an example of a large tetrahedral cage that exists in solution as a mixture of diastereomers, wherein the chirality of each iron(II) vertex influences only weakly the stereochemistry of its distant neighbors.[43−45] This stereochemical coupling may be enhanced, however, through the simple expedient of grafting methyl groups onto the terphenyl groups that form the cage's edges. Methylation thus gave rise to chiral communication[46−48] between vertices over a distance of ∼1.7 nm such that variations in the placement of the methyl groups allowed the system's delicately balanced thermodynamics to be perturbed to allow for the selection of either the homochiral *T* (ΔΔΔΔ/ΛΛΛΛ), the heterochiral C_3 (ΔΔΔΛ/ΛΛΛΔ), or the achiral S_4 (ΔΔΛΛ) cage diastereomer (Figure 1) as the self-assembly reaction's major product.

RESULTS AND DISCUSSION

The reaction between *p*-terphenylenediamine **A**, 2-formylpyridine, and iron(II) tetrafluoroborate in acetonitrile (Scheme 1) produced cage **1** as the only product observed by one- and two-dimensional NMR spectroscopy. Both the ^{1}H (Figure S1, Supporting Information) and ^{13}C (Figure S2) NMR spectra were complicated; NMR signals were observed as clusters of peaks, suggesting that **1** existed as a mixture of diastereomers in solution, in contrast to other cages prepared via subcomponent self-assembly.[27,34,35]

Evidence for the tetrahedral structure of **1** included $Fe_4L_6^{8+}$ and $Fe_4L_6(BF_4)^{7+}$ peaks in the FT-ICR (Fourier transform ion cyclotron resonance) mass spectrum, whose isotopic distribution corresponded well to calculated values (Figure S6), as well as the DOSY (diffusion-ordered spectroscopy)[49] spectrum of **1**, which showed that all peaks between 5.0 and 9.5 ppm had the same diffusion coefficient (Figure S7). The presence of an alternative structure, such as an $Fe_2L_3^{4+}$ triple helicate,[50−55] would lead to an increase in the intensity of every second peak in the ESI-MS signal for $Fe_4L_6^{8+}$ and the presence of DOSY peaks having different diffusion coefficients, neither of which was observed.

In order to quantify the amount of each diastereomer present in solution, the ^{1}H NMR peak clusters were deconvoluted using WINNMR[56] software (Figure 2a). Each diastereomer can give rise to different numbers of peaks in NMR spectra according to its symmetry: one set of ligand peaks for *T*, four sets for C_3, and three sets for S_4. Eight peaks are thus expected in total for each proton. When fewer than eight peaks were observed, we assumed

Received: June 7, 2011
Published: July 26, 2011

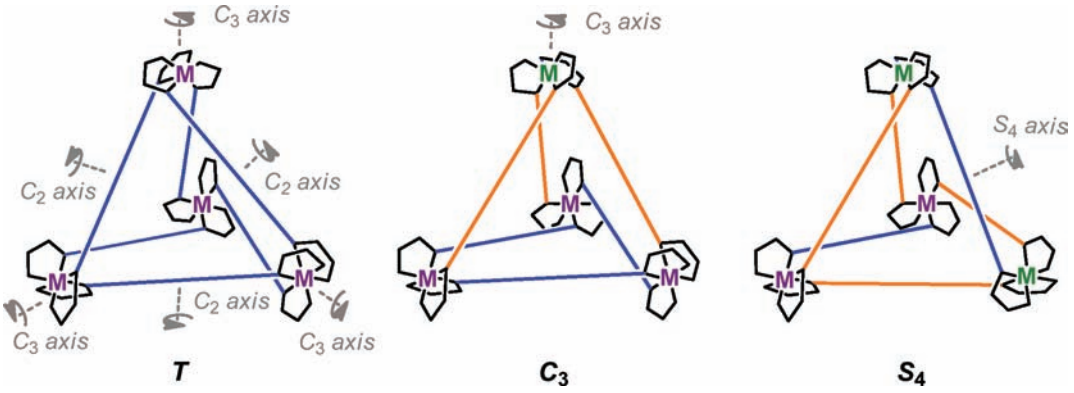

Figure 1. Schematic representations of the three possible diastereomers of M_4L_6 cages. Purple and green metal centers are of opposing chirality. Blue lines represent *anti*-linkages between homochiral metal centers, while orange lines represent *syn*-linkages between heterochiral metal centers.

Scheme 1. Synthesis of Tetrahedral Cage 1 (Major *T* Diastereomer Shown)

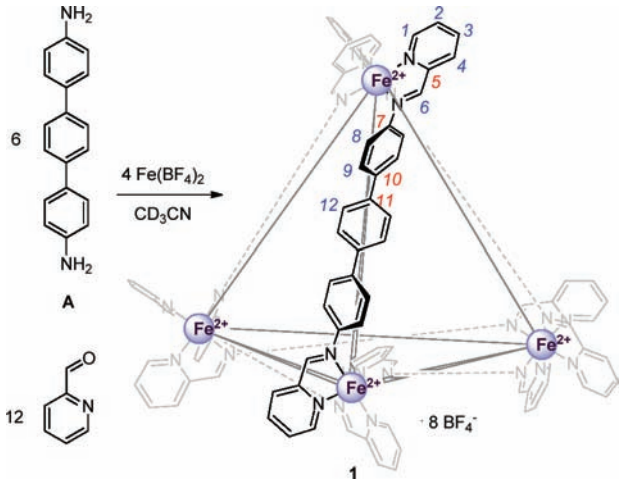

peak overlap. For example, the four possible ^{1}H resonances of **1**-C_3 were generally observed as three peaks in a 2:1:1 integrated ratio (see Supporting Information).

The three isomers of **1** were found to have nearly equal concentrations in solution, with the calculated percentages of 33%, 33%, and 34% for **1**-*T*, **1**-C_3, and **1**-S_4, respectively. This conclusion was further supported by similar analysis of the ^{13}C NMR spectrum of **1**, wherein C^{10} and C^8 (Scheme 1) were observed to give rise to all eight expected signals (Figure 2b). Analogous carbon atoms across the three diastereomers were observed to have similar T_1 values, allowing us to interpret the deconvolution of the ^{13}C peak clusters to obtain a diastereomeric distribution of 32%, 33%, and 35% for **1**-*T*, **1**-C_3, and **1**-S_4, in good quantitative agreement with the ^{1}H results. The CAChe[57] MM2-optimized structures of the three diastereomers of **1** were calculated to be nearly isoenergetic. The deviation of diastereomer populations from a statistical distribution (consisting of 12.5% *T*, 50% C_3, and 37.5% S_4) therefore reflects the presence of slight stereochemical coupling between metal centers.

In contrast to **1**, the great majority of tetrahedral M_4L_6 structures reported so far are homochiral, exhibiting strong stereochemical coupling between chiral metal centers,[39,43,58] including the

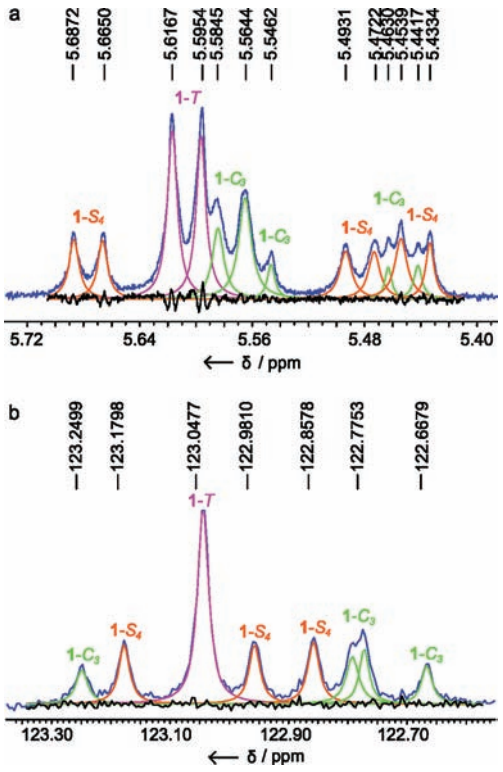

Figure 2. Deconvolution of peak clusters for (a) phenylene H^8 (^{1}H NMR spectrum) and (b) phenylene C^8 (^{13}C NMR spectrum) in **1**. The blue line is the measured spectrum. The orange, pink, and green lines are calculated Lorentzian peaks. The black line is the difference between the observed spectrum and the sum of all the Lorentzian peaks. A good fit should show only baseline noise.

three cages **2**−**4**[33−35,59] that have bis(iminopyridine) ligands of the same type as **1** (Figure 3).

We attribute the homochirality of cages **2**−**4** to stereochemical coupling between the metal centers mediated by the arylene rings that compose the cages' edges. Each of **2**−**4**[33−35,59] is built with a shorter biaryl bridge in place of **1**'s 4,4″-diaminoterphenyl; each of these ligands adopts an *anticlinal* conformation. In **2** the phenylene rings are observed to gear together next to the Fe^{II} centers with dihedral angles between terminal phenylene rings and the N−Fe−N chelate planes of 65 ± 7°.[19,35,60] In the crystal

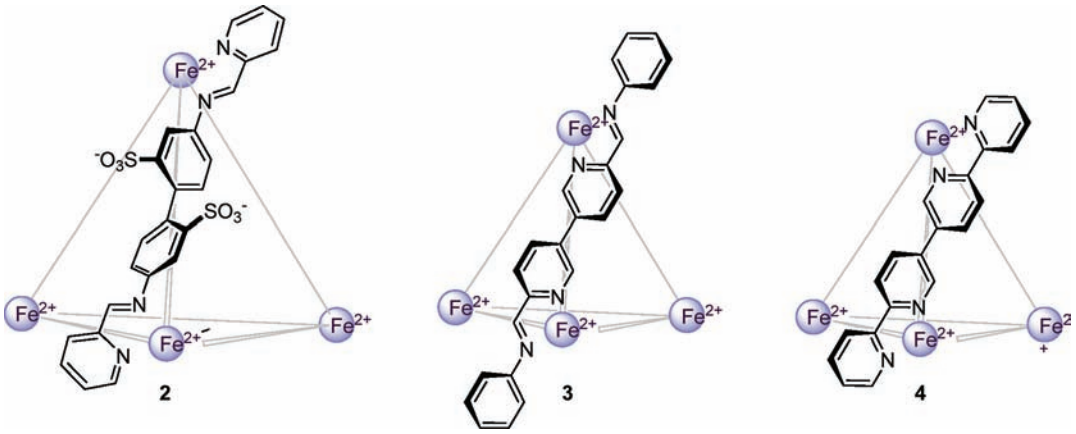

Figure 3. Previously reported homochiral bis(iminopyridine)-based $Fe^{II}_4L_4$ cages **2**,[35] **3**,[34] and **4**.[33,59]

structures of **3** and **4**, the pyridyl−pyridyl dihedral angles are about 57° (**3**) and 52° (**4**). The adoption of a *T*-symmetric structure allows these ligands to avoid either the transannular eclipsing of hydrogen atoms in **3** and **4** or steric and Coulombic interactions between sulfonates in **2**, necessitated by the coplanar arrangements in the *meso* arrangements of the ligands in the S_4 and C_3 diastereomers.

In order to test the hypothesis that stereochemical coupling[46−48] could be modulated in order to control the influence of the chirality of one Fe^{II} vertex upon its neighbors, methyl groups were introduced onto the terphenyl ligand backbone at various positions. The methyl group was chosen because its steric bulk has been demonstrated to constrain the conformations of biphenyl systems[61] and because methylated terphenyls are synthetically accessible. Three new C_2-symmetric methylated *p*-diaminoterphenyls were designed and synthesized (Scheme 2; synthetic details are given in the Supporting Information). The corresponding tetrahedral cages were prepared following the general synthetic method shown in Scheme 1 and characterized by NMR, ESI-MS, and elemental analysis.

The use of **B** led to the preparation of cage **5** as the uniquely observed product of the self-assembly reaction shown in Scheme 3. Both the ^{1}H (Figure 5a) and ^{13}C (Figure S9) NMR spectra of cage **5** appeared simpler than those of cage **1**. One major signal was observed for each ligand hydrogen or carbon atom, although in the ^{1}H spectrum each major peak was flanked by smaller peaks. Deconvolution analysis again suggested that three diastereomers, **5**-*T*, **5**-C_3, and **5**-S_4 were present. The ratio of isomers present, however, was different from that observed for **1**, with the proportion of the *T* isomer present doubling such that the **5**-*T*/**5**-C_3/**5**-S_4 ratio was observed to be 67%:23%:10%.

Vapor diffusion of diisopropyl ether into a nitromethane solution of cage **5** allowed the isolation of cube-shaped dark purple crystals suitable for X-ray analysis. Compound **5** crystallized in the monoclinic space group $P2_1/n$ with two cage molecules in the asymmetric unit. Each cage molecule is homochiral with either ΛΛΛΛ or ΔΔΔΔ configurations at the metal centers, and each has idealized *T* symmetry. The ligands bridging the metal centers adopt a helical twist with the helicity reflecting the handedness of the metal centers they bridge; Λ centers are linked by M-helices and Δ by P. Each ligand has an idealized *anti*-configuration. With ∼17 Å between adjacent metal centers, this species is among the largest M_4L_6 tetrahedra yet to be characterized by X-ray crystallography.[38,41,67−70] The two molecules in the asymmetric unit are enantiomers and interact via edge-to-face $\pi-\pi$ interactions. The methyl groups are located along the faces of the cage cavity. No anions, solvent, or significant electron density was located within the cage.

In the crystal structure of **5** (Figure 4), the three phenylene rings around each iron center are observed to twist out of planarity and conjugation with the imine groups to which they are bonded in order to avoid steric clash with each other and to benefit from weak CH···π stabilizing interactions between neighboring phenylenes. This twisting also allows the methyl groups to be directed toward the nearest-neighbor phenylene ring, in order to benefit from weak internal solvation and van der Waals stabilization.

When crystalline **5** was redissolved in CD_3CN, only one set of ^{1}H NMR signals was observed (Figure 5b), consistent with a stereochemically pure compound, **5**-*T*. The equilibrium mixture of diastereomers was regenerated after 5 days in solution at room temperature, resulting in a ^{1}H NMR spectrum indistinguishable from that of the freshly prepared cage.

Employing **C** (Scheme 2) in the subcomponent self-assembly reaction described for **5** yielded **6** (Scheme 4). In the ^{1}H NMR spectrum (Figure 6a) of **6**, a set of three peaks with equal relative integrated intensity is observed as the major signal for many protons, consistent with the presence of **6**-S_4 as the most abundant species in solution. NMR spectra revealed no detectable amounts of **6**-*T*; the relative abundances of **6**-S_4 and **6**-C_3 were thus measured to be 88% and 12% at room temperature. In contrast to **1** and **5** the peaks corresponding to both the terminal phenyl rings (Figure 6, δ 5.5−7 ppm) and the methyls were significantly broadened, suggesting that the terphenylene unit of the ligand as a whole rotates slowly on the NMR time scale.

Fine crystals of **6** (not suitable for X-ray crystallography) were obtained via liquid−liquid diffusion of diethyl ether into an acetonitrile solution. The recorded ^{1}H NMR spectrum of freshly dissolved crystals showed the S_4 isomer only (Figure 6b). Monitoring the decrease of **6**-S_4 in solution by ^{1}H NMR spectroscopy over 12 h at 298 K revealed a gradual return to the equilibrium population of the S_4 and C_3 isomers (Figure 6c) with a rate constant for conversion of **6**-S_4 to **6**-C_3 of $(7.1 \pm 0.7) \times 10^{-6}$ s^{-1}, corresponding to an activation barrier, $\Delta G^{\ddagger}$, of 102 kJ mol^{-1} at 298 K.

This behavior for cage **6** is similar to what was observed for cage **5**: one isomer crystallized preferentially, with possible elimination

Scheme 2. Synthetic Routes to the New Methylated Diaminoterphenyls B, C, and D[a]

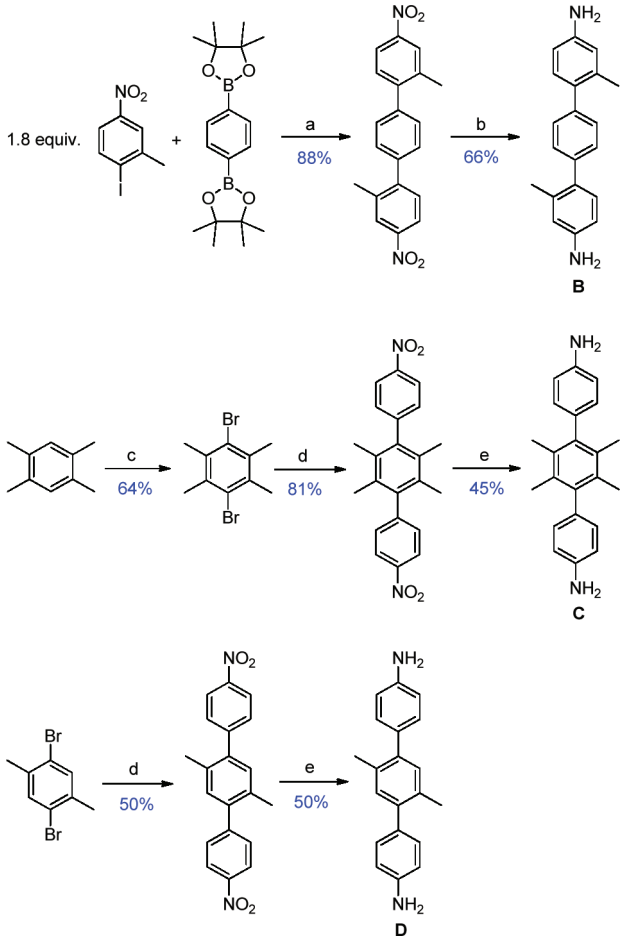

[a] Conditions: (a) 2 equiv of Ag_2CO_3, 0.05 equiv of $Pd(PPh_3)_4$, THF, Dean−Stark trap, reflux in the dark, 1 day;[62] (b) H_2, 1 atm, 0.1 equiv of 10% Pd/C, EtOAc, room temp, 1.5 days;[63] (c) 0.02 equiv of I_2, 2.5 equiv of Br_2, DCM, reflux, 1.5 h;[64] (d) 2.5 equiv of 4-nitrobenzene boronic acid, 0.1 equiv of $Pd(PPh_3)_4$, 5 equiv of Cs_2CO_3, 1,4-dioxane/H_2O 5:1, reflux, 12 h;[65] (e) 50 equiv of $N_2H_4 \cdot H_2O$, 0.1 equiv of 10% Pd/C, EtOH, reflux, 12 h.[66]

of the less-symmetric isomers from the dynamic library[71,72] of diastereomers in solution during crystallization, as we have observed in the case of a chiral dicopper helicate.[73]

Cage **7** was synthesized from diamine **D** (Scheme 5) under conditions analogous to those used in the preparation of **1**, **5**, and **6**. The ^{1}H NMR spectrum of **7** (Figure 7) revealed a mixture of three diastereomers, with the ratio **7**-*T*/**7**-C_3/**7**-S_4 measured to be 21.4%:43.9%:34.7%, indicating a preference for the C_3 diastereomer over *T* compared to nonmethylated **1**.

Factors Governing Stereocontrol. Figure 8 summarizes the differences in diastereoselectivity observed between the four terphenyl-edged Fe_4L_6 cages reported in this study, as measured at equilibrium, when ^{1}H NMR analysis revealed no further changes in diastereomeric ratios (in all cases within 24 h at 298 K). Whereas nonmethylated **1** gave nearly equal proportions of the three diastereomers, methylation on the terminal phenylene rings (**5**) favored the *T*-diastereomer, tetramethylation on the central ring (**6**) favored S_4, and dimethylation on the central phenylene (**7**) favored C_3.

Scheme 3. Synthesis of $Fe^{II}_4L_6$ Cage 5 (Major *T* Diastereomer Shown)

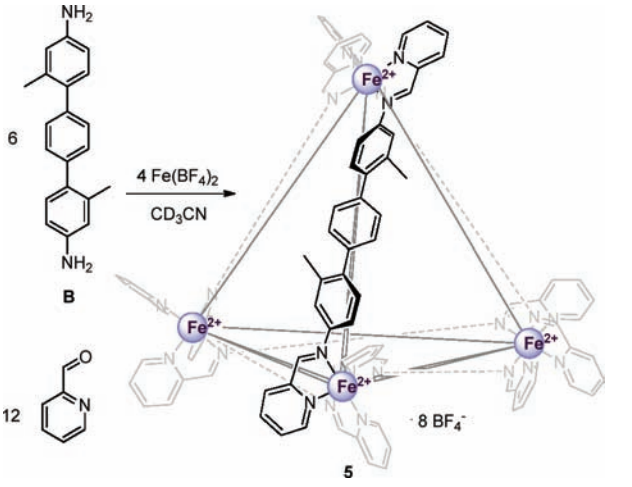

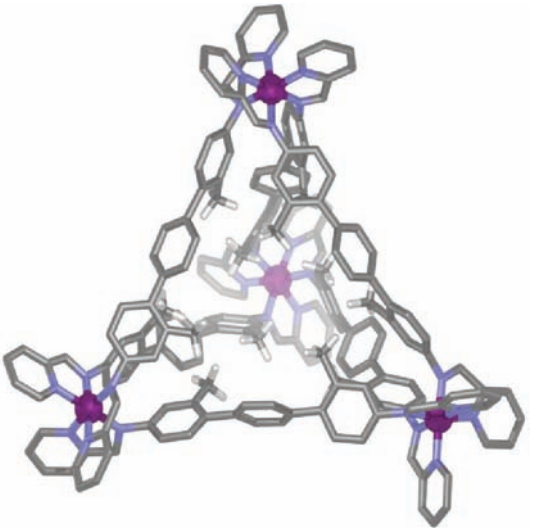

Figure 4. Schematic representation of the crystal structure of the ΔΔΔΔ enantiomer of **5**-*T*. For clarity, anions and solvent of crystallization are removed and only methyl hydrogen atoms are shown.

The thermodynamics of these cages are more finely balanced than what has been observed previously in the cases of homochiral cages **2**−**4** (Figure 3). The diastereoselectivities observed in the present system reflect energetic differences of 1−10 kJ mol^{-1} between diastereomers, similar to what might be observed between diastereomeric transition states leading to the two product enantiomers of a diastereoselective reaction.[43] Understanding the subtle factors that underlie the transfer of stereochemical information within cages of this type may help to shed light upon the mechanism of stereoselective transformations,[74−77] as well as more fundamental questions of chiral information transfer.[46,78−81]

As shown in Figure 1, each ligand within an M_4L_6 cage bridges two metal centers either of the same chirality in *anti* fashion or of opposite chiralities in *syn* fashion. These two ligand conformations are shown in Figure 9a and Figure 9b. Factors that favor a *syn* ligand conformation also favor the S_4 and C_3 diastereomers,

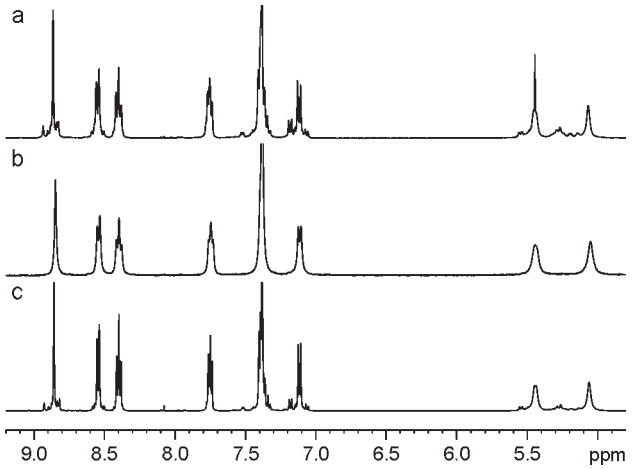

Figure 5. Comparison of ^{1}H NMR spectra of cage **5** in CD_3CN (all recorded at 298 K): (a) **5** formed as shown in Scheme 2; (b) crystals of **5** 10 min after dissolution; (c) 5 days after dissolution.

Scheme 4. Synthesis of Tetrahedral Cage 6 (Major S_4 Diastereomer Shown)[a]

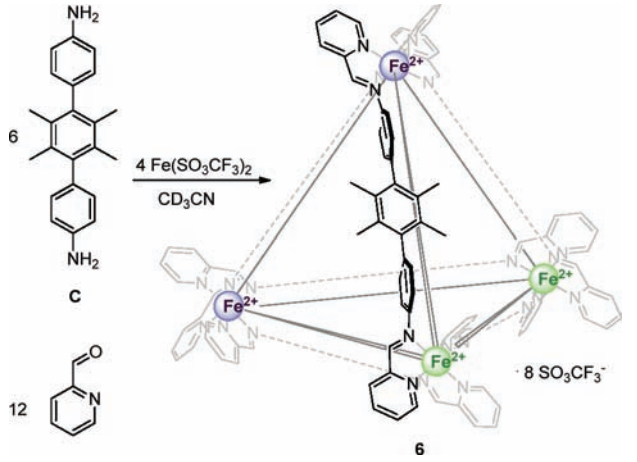

[a] Green Fe^{II} centers are of opposite handedness to those colored purple.

which contain four and three *syn*-bridging ligands respectively, whereas factors that favor an *anti* ligand conformation favor the *T* diastereomer, which contains only *anti* ligands. The stereochemical coupling phenomena that favor either the *syn* or *anti* configuration within the terphenylenediamine subcomponents **A**−**D** are discussed below.

In the crystal structure of **5** the dihedral angles between the N−Fe−N chelate planes and terminal phenyl rings average 74 ± 7° (Figure 9a); the average of all 84 analogous dihedrals for structures containing similar *fac*-coordinated iron(II) tris-(2-pyridyl-phenylimine) motifs reported in the 2011 Cambridge Structural Database[82] is 69 ± 9°, suggesting that these dihedrals are not strained in **5**. Each central phenylene in **5** thus lies at a 60 ± 9° dihedral angle to each of its neighbors, close to the optimal value of 55° for the parent dimethylterphenyl.[83] All dihedral angles in the *anti* ligands of the *T* diastereomer of **5** thus lie close to optimal values, with each ligand taking on a chiral twist between metal ions.

The *syn* ligand orientation required to generate S_4 and C_3 cage diastereomers (Figure 9b), in contrast, approximates a *meso*

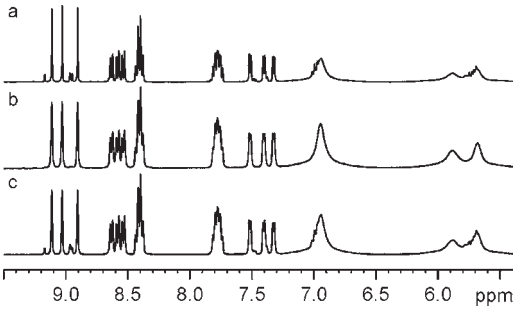

Figure 6. Comparison of ^{1}H NMR spectra of cage **6** (only the aromatic region is shown, all recorded at 298 K): (a) **6** formed as shown in Scheme 3; (b) crystals of **6** 5 min after dissolution; (c) 12 h after dissolution.

Scheme 5. Synthesis of Tetrahedral Cage 7 (Major C_3 Diastereomer Shown)[a]

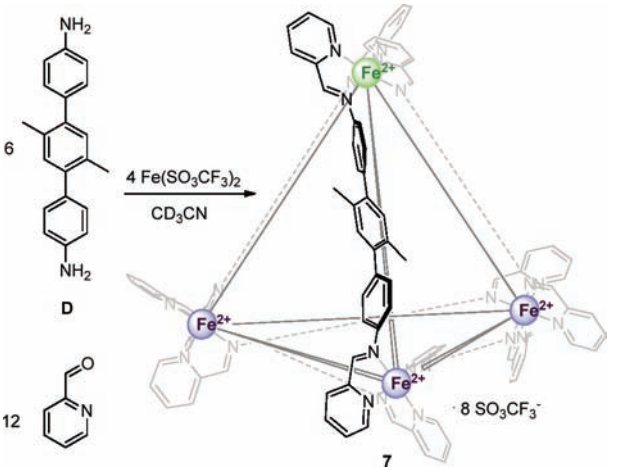

[a] The green Fe^{II} center is of opposite handedness to those colored purple.

configuration between two metal ions of opposite handedness. Although this configuration does not preclude the central phenylene from lying at an optimal 55° angle to both of the terminal phenyls, the required *cis* orientation of the methyl groups appears to be very slightly disfavored with respect to the *trans* methyl orientation of the *anti* ligands of **5**-*T*.[83] In order to adopt such a *trans* orientation, the methyl groups would need to break van der Waals contact with neighboring phenyl rings. This frustrated state thus appears to raise slightly the energy of the *syn* ligand conformation, and thus the **5**-C_3 or **5**-S_4 diastereomers, with respect to the *anti* ligand conformation and the **5**-*T* diastereomer.

In the parent (tetramethyl)terphenylene of diamine **C**, the steric bulk of the four methyl groups situated on its central phenylene ring obliges the two terminal phenylene rings to lie orthogonal to the central ring, and thus coplanar with each other, in the lowest-energy conformation.[84] In such a coplanar arrangement, tight gearing between the terminal phenylene groups precludes them both from adopting an optimal 74° dihedral angle to two imines linked to Fe^{II} centers of the same handedness (as in Figure 9a). In the *meso* configuration imposed by a *syn* linkage (Figure 9b), however, any dihedral angle may be adopted between the terminal phenyl groups and the imines linked to Fe^{II}

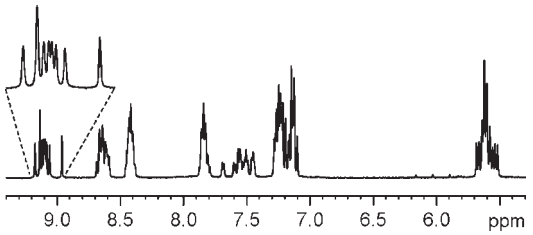

Figure 7. ^{1}H NMR spectrum for cage **7** (recorded at 313 K after the system was observed to have reached equilibrium; only the aromatic region is shown) with an expansion of the imine region.

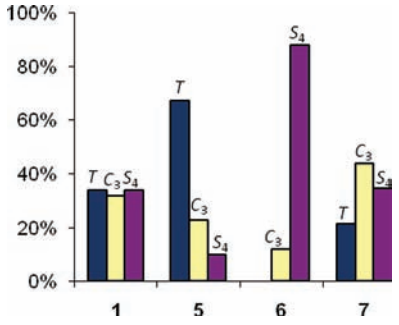

Figure 8. Equilibrium distribution of diastereomers for cages **1**, **5**, **6**, and **7** at 298 K.

centers of opposite handedness; these dihedrals are the isoenergetic mirror images of each other. The *syn* arrangement and thus the S_4 and to a lesser degree the C_3 diastereomers are therefore favored for any ligand whose terminal phenyl groups are coplanar in the lowest-energy conformation, as with **6**.

The parent diaminoterphenyl **D**, whose central phenylene group bears two methyl groups, also shows coplanarity between its terminal phenyl groups in the lowest-energy conformation.[85] The central ring is not obliged to lie orthogonal to the two terminal rings, however, allowing the ligands of **7** readily to adopt either a *syn* or *anti* configuration. As a result, the observed population of isomers in solution approaches the statistical ratio, as with cage **1**, with a slightly lower predominance of the *T* diastereomer and an increase of the C_3-symmetry diastereomer in the case of **7**, possibly as the result of a slight favoring of the *syn* configuration.

In summary, the use of diamine ligands that preferentially adopt an *anti* arrangement, as in cage **5**, should lead to the preferential formation of homochiral *T*-symmetric cages, which contain all *anti* ligands. The use of ligands that preferentially adopt a *syn* arrangement, such as the *meso*-favoring ligands of cage **6**, should lead to the preferential formation of S_4-symmetric cages, which contain mostly ligands in this orientation. The lowest-symmetry C_3 diastereomer is favored on statistical grounds and will prevail at the expense of the *T* diastereomer if a slight *syn* bias is applied, as in the case of cage **7**.

Variable Temperature Behavior. The equilibrated states of cages **1**, **5**, **6**, and **7** in acetonitrile at 10 different temperatures ranging from 298 to 343 K were studied. Equilibration was monitored by ^{1}H NMR spectroscopy; each system was noted to have reached equilibrium when its NMR spectrum no longer changed. In contrast with other M_4L_6 tetrahedra reported in the literature,[41,43] no coalescence was observed for any of these cages up to 343 K, suggesting that the activation barrier to racemization of the Fe^{II} stereocenters

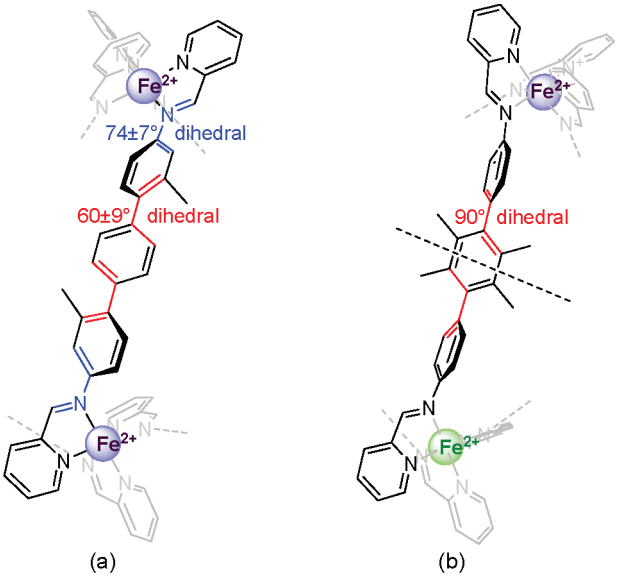

Figure 9. Two linking modes: (a) an *anti* ligand connecting two Fe^{II} centers with the same stereochemistry in **5**; (b) a *syn* ligand connecting two Fe^{II} centers with opposite stereochemistry in **6**, showing the pseudo-mirror plane.

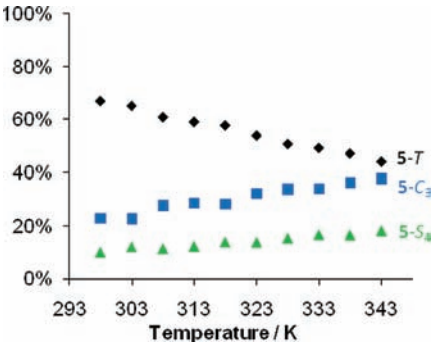

Figure 10. Temperature dependence of diastereomer distribution for cage **5**.

was greater than 85 kJ mol^{-1}, consistent with the barrier to diastereomer interconversion of 102 kJ mol^{-1} for **6** at 298 K, as noted above. The mechanism of racemization of Fe(diimine)$_3$ centers has been reported to involve a combination of predominantly intramolecular (Rây-Dutt twist or Bailar twist) and minor intermolecular (dissociative) rearrangements. The interconversion barriers observed in the present systems are consistent with these prior reports, suggesting a predominantly intramolecular isomerization process.[43,86−89] The molar percentages of each diastereomer for each cage at equilibrium were calculated and compared at different temperatures. As the temperature was increased, the population of **5**-*T* decreased gradually as the populations of both **5**-C_3 and **5**-S_4 were observed to increase (Figure 10); in contrast, no significant changes in diastereomer populations were observed for cages **1**, **6**, and **7**. Van't Hoff analysis for the equilibrium **5**-*T* ⇄ **5**-C_3 (presented in the Supporting Information) revealed enthalpic and entropic contributions of ΔH = 19 kJ mol^{-1} and ΔS = 54 J K^{-1} mol^{-1}, respectively, whereas those for **1**, **6**, and **7** are minimal (ΔH <7 kJ mol^{-1}, ΔS <18 J K^{-1} mol^{-1}).

The temperature dependence of the diastereomeric interconversion of **5** is a consequence of the greater entropy change associated with this process. Each of **5**'s methyl groups may independently be oriented either inward, as all are observed to point in the crystal structure (Figure 4), or outward, following a 180° rotation of the imine−phenylene dihedral. An outward orientation would disrupt the weak van der Waals interaction between a methyl group and the phenyl group of its neighboring ligand, leading to a disruption of the stereochemical coupling effects to which we attribute the stereoinduction observed in **5**. More fundamentally, we would expect that for **5** and indeed for any system in which the *T* diastereomer is favored at lower temperatures, the amount of the most ordered and thus most entropically disfavored *T* should decrease in favor of the more entropically favored S_4 and C_3 diastereomers as the temperature increases.

CONCLUSIONS

Our recently developed tetrahedral-cage-forming procedure[35] thus proved extendable to the preparation of larger structures. These structures formed cleanly but exhibited complex stereoisomery, controllable through the introduction of methyl groups onto the linear diamine subcomponent. This work thus builds upon, and contributes to, fundamental studies of the transfer of chiral information between subunits of larger systems,[78,79,81,90,91] which has been shown to underlie such complex phenomena as creating twisted ribbons from self-assembling dendrons,[92] fixing the stereochemistry of a photocycloaddition reaction product within a subtly chiral host,[23] determining the direction of travel within a mechanically interlocked molecular machine,[93] and converting light energy into macroscopic rotational motion.[94] The ability to manipulate diastereomer distribution offered by this study provides an additional means to exert control over the form of a host's inner phase.[95] As enantiomerically defined cages have provided useful chiral spaces for enantioselective catalysis and the differential molecular recognition of enantiomers,[22,23,39,40,67,96] so may diastereomerically defined cages permit the discrimination and transformation of diastereomeric guests.

EXPERIMENTAL SECTION

General. Chromatographic separations were performed on silica gel 60 (particle size 0.040−0.063 mm) purchased from Breckland Scientific Supplies. TLC was performed on silica gel 60 F254 purchased from Merck; visualization was under ultraviolet light (ν = 254 nm). ^{1}H NMR spectra were recorded at 400 MHz. ^{13}C NMR, ^{1}H−^{1}H COSY, ^{1}H−^{13}C HMQC (heteronuclear multiple quantum coherence), DEPT-135 (distortionless enhancement by polarization transfer at pulse angle θ = 135°), and DOSY (diffusion-ordered spectroscopy) spectra were recorded on a 500 MHz spectrometer. NMR spectra were referenced to the residual ^{1}H or ^{13}C NMR signal of the solvent.[97] Electrospray ionization mass spectra were obtained on a Micromass Quattro LC instrument, infused from a Harvard syringe pump at a rate of 10 μL per minute. Mass spectra provided by the EPSRC National Mass Spectrometry Service Centre at Swansea, U.K., were acquired on a Thermofisher LTQ Orbitrap XL. Satisfactory elemental analyses required the inclusion of water molecules; this water was observed in ^{1}H NMR spectra of crystallized products. Possible sources of water include the imine condensation reaction and the solvents employed. The syntheses of terphenylenediamines **B**−**D** are reported in the Supporting Information.

Crystallography. Data for **5** were collected on a Bruker-Nonius APEX2-X8-FR591 diffractometer employing confocal mirror monochromated Mo Kα radiation generated from a rotating anode (0.710 73 Å) with ω and ψ scans to approximately 46° 2θ at 120(2) K.[98] Data integration and reduction were undertaken with S HKL Denzo and Scalepack.[98,99] Subsequent computations were carried out using the WinGX-32 graphical user interface.[100] Structures were solved by direct methods using SIR97.[101] Multiscan empirical absorption corrections were applied to the data set using the program SADABS.[102] Data were refined and extended with SHELXL-97.[103] Hydrogen atoms were refined using a riding model with the hydrogens on the methyl groups modeled as disordered over two positions. The crystals diffracted poorly and rapidly suffered solvent loss. Despite rapid handling times and a low temperature collection, the quality of data was less than ideal. Because of the low quality of the data, numerous rigid body restraints were required in the phenyl and pyridyl rings and only the iron atoms were refined anisotropically. Nevertheless, the quality of the data is more than sufficient for establishing the connectivity of the structure. The anions and nitromethane solvent of crystallization within the lattice were significantly disordered, and they could not be successfully modeled. Therefore, the SQUEEZE function of PLATON[104] was employed to remove the contribution of the electron density associated with these anions and solvent from the model, which resulted in far more satisfactory residuals.

Crystallographic data for **5** are as follows: formula $C_{212}H_{216}B_8F_{32}Fe_4N_{44}O_{40}$, M = 4938.16, monoclinic, space group $P2_1/n$ (No. 14), a = 32.3941(19) Å, b = 47.504(3) Å, c = 36.205(2) Å, β = 104.098(2)°, V = 54036(6) Å^3, D_c = 1.214 g cm^{-3}, Z = 8, crystal size 0.41 mm × 0.36 mm × 0.16 mm, color purple, habit block, temperature 120(2) K, λ(Mo Kα) = 0.71073 Å, μ(Mo Kα) = 0.302 mm^{-1}, T(SADABS)$_{min,max}$ of 0.4904 and 0.7452, 2θ_{max} = 31.72, *hkl* range from −24 to 24, from −36 to 36, and from −27 to 26, N = 123856, N_{ind} = 24261 (R_{merge} = 0.1020), N_{obs} = 13 465 ($9I > 2\sigma(I)$), N_{var} = 1066, residuals $R_1(F)$ = 0.1354, wR2(F^2) = 0.3726, GoF(all) = 1.176, D$\rho_{min,max}$ of −0.345 and 0.398 e Å^{-3}.

Cage 1. To a Teflon-stoppered NMR tube was added 4,4″-diamino-*p*-terphenyl (2.60 mg, 10 μmol, 6 equiv), 2-pyridinecarboxaldehyde (1.9 μL, 2.14 mg, 20 μmol, 12 equiv), iron(II) tetrafluoroborate hexahydrate (2.25 mg, 6.7 μmol, 4 equiv), and deuterated acetonitrile (0.5 mL). The solution was degassed by three evacuation/N_2 fill cycles. The tube was kept at 50 °C overnight. ^{1}H NMR (CD_3CN, 400 MHz, for atom assignments see Scheme 1): 8.97−8.82 (12H, imine H^6), 8.58−8.51 (12H, py-H^4), 8.35−8.44 (12H, py-H^3), 7.95−7.83 (24H, Ph-H^{12}), 7.83−7.69 (12H, py-H^2), 7.69−7.49 (24H, Ph-H^9), 7.49−7.36 (12H, py-H^1), 5.66−5.41 (24H, Ph-H^8). ^{13}C {^{1}H} NMR (125 MHz, CD_3CN): 175.87−175.19 (12C, C^6), 159.31−159.03 (12C, C^5), 157.07−156.52 (12C, C^1), 150.81−150.48 (12C, C^7), 141.22−141.03 (12C, C^{11}), 140.76−140.60 (12C, C^3), 139.81−139.31 (12C, C^{10}), 132.28−131.96 (12C, C^4), 130.95−130.68 (12C, C^2), 128.72−128.30 (36C, C^{12} and C^9), 123.25−122.67 (24C, C^8). FT-ICR MS: $[Fe_4L_6]^{8+}$ 356.86, $[Fe_4L_6(BF_4)]^{7+}$ 420.12. Found: C, 59.21; H, 4.02; N, 9.38%. Calcd for $C_{180}H_{132}B_8F_{32}Fe_4N_{24}\cdot 6H_2O\cdot CH_3CN$: C, 59.11; H, 4.01; N, 9.47%.

Cage 5. To a Teflon capped NMR tube was added diamine **B** (11.4 mg, 39.5 μmol, 6 equiv), 2-pyridinecarboxaldehyde (7.56 μL, 8.47 mg, 79.1 μmol, 12 equiv), iron(II) tetrafluoroborate hexahydrate (8.89 mg, 26.4 μmol, 4 equiv), and deuterated acetonitrile (0.5 mL). The solution was degassed by three evacuation/N_2 fill cycles. The tube was kept at 50 °C overnight. The product was purified by recrystallization: diethyl ether was diffused into an acetonitrile solution of the cage. The desired product methyl cage **5** was isolated by filtration as purple solid (11 mg, 45%). ^{1}H NMR (CD_3CN, 500 MHz): 8.85 (12H, s, imine *H*), 8.54 (12H, d, *J* 7.5, py-*H*), 8.39 (12H, t, *J* 7.5, py-*H*), 7.75 (12H, t, *J* 6.25, py-*H*), 7.38 (36H, py-*H* and Ph-*H*), 7.11 (12H, d, *J* 8.0, Ph-*H*), 4.9−5.6 (24H, br, Ph-*H*), 5.06 (12H, s, Ph-*H*), 1.90 (36H, s, CH_3). ^{13}C {^{1}H} NMR (125 MHz, CD_3CN): 175.3, 159.3, 156.7, 150.2, 140.6, 140.2, 137.9, 131.7, 131.2, 130.5, 129.8, 123.7, 119.6, 20.57. ESI-MS: $[Fe_4L_6]^{8+}$ 377.74, $[Fe_4L_6(BF_4)]^{7+}$ 444.23. Found: C, 58.14; H, 4.54; N, 8.29%. Calcd for $C_{192}H_{156}B_8F_{32}Fe_4N_{24}\cdot 14H_2O$: C, 58.09; H, 4.67; N, 8.47%.

Cage 6. To a Teflon capped NMR tube was added diamine **C** (8 mg, 25.3 μmol, 6 equiv), 2-pyridinecarboxaldehyde (4.8 μL, 5.4 mg, 50.6 μmol, 12 equiv), iron(II) trifluoromethanesulfonate (6.0 mg, 16.8 μmol, 4 equiv), and deuterated acetonitrile (0.5 mL). The solution was degassed by three evacuation/N_2 fill cycles. The tube was kept at 50 °C overnight. The product was purified by recrystallization: diethyl ether was diffused into an acetonitrile solution of the cage. The desired product methyl cage **6** was isolated by filtration as purple solid (12 mg, 65%). ^{1}H NMR (CD_3CN, 400 MHz): 8.90−9.16 (12H, imine *H*), 8.52−8.65 (12H, py-*H*), 8.37−8.43 (12H, py-*H*), 7.73−7.82 (12H, py-*H*), 7.31−7.52 (12H, py-*H*), 6.80−7.00 (24H, Ph-*H*), 5.60−6.00 (24H, Ph-*H*), 1.70−2.20 (36H, CH_3). ^{13}C {^{1}H} NMR (125 MHz, CD_3CN): 175.7−176.2, 159.2−159.3, 156.4−156.9, 150.0−150.7, 143.4−144.1, 140.5−141.1, 130.7−133.0, 120.7−123.3, 19.0 (12C, CH_3). ESI-MS: $[Fe_4L_6]^{8+}$ 398.82, $[Fe_4L_6(CF_3SO_3)]^{7+}$ 477.12, $[Fe_4L_6(CF_3SO_3)_2]^{6+}$ 581.42. Found: C, 56.33; H, 4.10; N, 7.31%. Calcd for $C_{212}H_{180}F_{24}Fe_4N_{24}O_{24}S_8 \cdot 8H_2O$: C, 56.24; H, 4.36; N, 7.42%.

Cage 7. To a Teflon capped NMR tube was added diamine **D** (6.4 mg, 22.2 μmol, 6 equiv), 2-pyridinecarboxaldehyde (4.2 μL, 4.7 mg, 44.4 μmol, 12 equiv), iron(II) trifluoromethanesulfonate (5.3 mg, 14.8 μmol, 4 equiv), and deuterated acetonitrile (0.5 mL). The solution was degassed by three evacuation/N_2 fill cycles. The tube was kept at 50 °C overnight. The product was purified by recrystallization: diethyl ether was diffused into an acetonitrile solution of the cage. The desired product methyl cage **7** was isolated by filtration as purple solid (8 mg, 51%). ^{1}H NMR (CD_3CN, 500 MHz): 8.87−9.00 (12H, imine *H*), 8.52−8.61 (12H, py-*H*), 8.37−8.41 (12H, py-*H*), 7.74−7.78 (12H, py-*H*), 7.33−7.55 (12H, py-*H*), 7.08−7.25 (36H, Ph-*H*), 5.47−5.60 (24H, Ph-*H*), 2.17−2.28 (36H, CH_3). ^{13}C {^{1}H} NMR (125 MHz, CD_3CN): 176.0−175.4, 159. 4−159.0, 157.0−156.5, 150.4−150.0, 142.8−142.6, 141.0−140.4, 134.0−133.5, 132.7−131.9, 131.2−130.6, 122.5−121.9, 20.2−19.8. ESI-MS: $[Fe_4L_6]^{8+}$ 377.75, $[Fe_4L_6(CF_3SO_3)]^{7+}$ 453.07, $[Fe_4L_6(CF_3SO_3)_2]^{6+}$ 553.39. Found: C, 54.20; H, 3.77; N, 7.23%. Calcd for $C_{200}H_{156}F_{24}Fe_4N_{24}O_{24}S_8 \cdot 12H_2O$: C, 54.21; H, 4.09; N, 7.59%.

■ ASSOCIATED CONTENT

Supporting Information. Synthetic procedures, NMR spectra and deconvolution analyses, Van't Hoff analyses, kinetics data and analysis, MS data, crystal structure data for **5**. This material is available free of charge via the Internet at http://pubs.acs.org.

■ AUTHOR INFORMATION

Corresponding Author
jrn34@cam.ac.uk

■ ACKNOWLEDGMENT

This work was supported by the Walters-Kundert Charitable Trust, the Marie Curie Incoming International Fellowship Scheme of the 7th EU Framework Program (J.K.C.), and the UK Engineering and Physical Sciences Research Council (EPSRC). We thank the EPSRC National Mass Spectrometry Service at Swansea, U.K., for FT-ICR MS experiments and the National Crystallography Service at Southampton for collecting X-ray data.

■ REFERENCES

(1) Ward, M. D. *Chem. Commun.* **2009**, 4487–4499.
(2) Dalgarno, S. J.; Power, N. P.; Atwood, J. L. *Coord. Chem. Rev.* **2008**, *252*, 825–841.
(3) Fujita, M.; Tominaga, M.; Hori, A.; Therrien, B. *Acc. Chem. Res.* **2005**, *38*, 369–378.
(4) Saalfrank, R. W.; Maid, H.; Scheurer, A. *Angew. Chem., Int. Ed.* **2008**, *47*, 8794–8824.
(5) Tranchemontagne, D. J.; Ni, Z.; O'Keeffe, M.; Yaghi, O. M. *Angew. Chem., Int. Ed.* **2008**, *47*, 5136–5147.
(6) Seidel, S. R.; Stang, P. J. *Acc. Chem. Res.* **2002**, *35*, 972–983.
(7) Ghosh, K.; Hu, J.; White, H. S.; Stang, P. J. *J. Am. Chem. Soc.* **2009**, *131*, 6695–6697.
(8) Zheng, Y.-R.; Zhao, Z.; Kim, H.; Wang, M.; Ghosh, K.; Pollock, J. B.; Chi, K.-W.; Stang, P. J. *Inorg. Chem.* **2010**, *49*, 10238–10240.
(9) Yoshizawa, M.; Klosterman, J. K.; Fujita, M. *Angew. Chem., Int. Ed.* **2009**, *48*, 3418–3438.
(10) Koblenz, T. S.; Wassenaar, J.; Reek, J. N. H. *Chem. Soc. Rev.* **2008**, *37*, 247–262.
(11) Breiner, B.; Clegg, J. K.; Nitschke, J. R. *Chem. Sci.* **2011**, *2*, 51–56.
(12) Yoshizawa, M.; Tamura, M.; Fujita, M. *Science* **2006**, *312*, 251–254.
(13) Pluth, M. D.; Bergman, R. G.; Raymond, K. N. *Science* **2007**, *316*, 85–88.
(14) Hastings, C. J.; Fiedler, D.; Bergman, R. G.; Raymond, K. N. *J. Am. Chem. Soc.* **2008**, *130*, 10977–10983.
(15) Kuil, M.; Soltner, T.; Van Leeuwen, P. W. N. M.; Reek, J. N. H. *J. Am. Chem. Soc.* **2006**, *128*, 11344–11345.
(16) Furutani, Y.; Kandori, H.; Kawano, M.; Nakabayashi, K.; Yoshizawa, M.; Fujita, M. *J. Am. Chem. Soc.* **2009**, *131*, 4764–4768.
(17) Yoshizawa, M.; Miyagi, S.; Kawano, M.; Ishiguro, K.; Fujita, M. *J. Am. Chem. Soc.* **2004**, *126*, 9172–9173.
(18) Dong, V. M.; Fiedler, D.; Carl, B.; Bergman, R. G.; Raymond, K. N. *J. Am. Chem. Soc.* **2006**, *128*, 14464–14465.
(19) Mal, P.; Breiner, B.; Rissanen, K.; Nitschke, J. R. *Science* **2009**, *324*, 1697–1699.
(20) Sawada, T.; Yoshizawa, M.; Sato, S.; Fujita, M. *Nat. Chem.* **2009**, *1*, 53–56.
(21) Yoshizawa, M.; Tamura, M.; Fujita, M. *Angew. Chem., Int. Ed.* **2007**, *46*, 3874–3876.
(22) Fiedler, D.; Leung, D. H.; Bergman, R. G.; Raymond, K. N. *J. Am. Chem. Soc.* **2004**, *126*, 3674–3675.
(23) Nishioka, Y.; Yamaguchi, T.; Kawano, M.; Fujita, M. *J. Am. Chem. Soc.* **2008**, *130*, 8160–8161.
(24) Ziegler, M.; Davis, A. V.; Johnson, D. W.; Raymond, K. N. *Angew. Chem., Int. Ed.* **2003**, *42*, 665–668.
(25) Abrahams, B. F.; Egan, S. J.; Robson, R. *J. Am. Chem. Soc.* **1999**, *121*, 3535–3536.
(26) Bell, Z. R.; Harding, L. P.; Ward, M. D. *Chem. Commun.* **2003**, 2432–2433.
(27) Meng, W.; Breiner, B.; Rissanen, K.; Thoburn, J. D.; Clegg, J. K.; Nitschke, J. R. *Angew. Chem., Int. Ed.* **2011**, *50*, 3479–3483.
(28) Roche, S.; Haslam, C.; Heath, S. L.; Thomas, J. A. *Chem. Commun.* **1998**, 1681–1682.
(29) Stephenson, A.; Ward, M. D. *Dalton Trans.* **2011**, *40*, 7824–7826.
(30) Sun, Q.-F.; Iwasa, J.; Ogawa, D.; Ishido, Y.; Sato, S.; Ozeki, T.; Sei, Y.; Yamaguchi, K.; Fujita, M. *Science* **2010**, *328*, 1144–1147.
(31) Albrecht, M.; Janser, I.; Frohlich, R. *Chem. Commun.* **2005**, 157–165.
(32) Caulder, D. L.; Powers, R. E.; Parac, T. N.; Raymond, K. N. *Angew. Chem., Int. Ed.* **1998**, *37*, 1840–1843.
(33) Glasson, C. R. K.; Meehan, G. V.; Clegg, J. K.; Lindoy, L. F.; Turner, P.; Duriska, M. B.; Willis, R. *Chem. Commun.* **2008**, 1190–1192.
(34) Hristova, Y. R.; Smulders, M. M. J.; Clegg, J. K.; Breiner, B.; Nitschke, J. R. *Chem. Sci.* **2011**, *2*, 638–641.
(35) Mal, P.; Schultz, D.; Beyeh, K.; Rissanen, K.; Nitschke, J. R. *Angew. Chem., Int. Ed.* **2008**, *47*, 8297–8301.
(36) Saalfrank, R. W.; Stark, A.; Peters, K.; von Schnering, H. G. *Angew. Chem., Int. Ed. Engl.* **1988**, *27*, 851–853.

(37) Stang, P. J.; Olenyuk, B.; Muddiman, D. C.; Smith, R. D. *Organometallics* **1997**, *16*, 3094–3096.
(38) Tidmarsh, I. S.; Taylor, B. F.; Hardie, M. J.; Russo, L.; Clegg, W.; Ward, M. D. *New J. Chem.* **2009**, *33*, 366–375.
(39) Argent, S. P.; Riis-Johannessen, T.; Jeffery, J. C.; Harding, L. P.; Ward, M. D. *Chem. Commun.* **2005**, 4647–4649.
(40) Albrecht, M.; Burk, S.; Weis, P. *Synthesis* **2008**, 2963–2967.
(41) Saalfrank, R. W.; Demleitner, B.; Glaser, H.; Maid, H.; Bathelt, D.; Hampel, F.; Bauer, W.; Teichert, M. *Chem.—Eur. J.* **2002**, *8*, 2679–2683.
(42) Cotton, F. A.; Murillo, C. A.; Yu, R. *Dalton Trans* **2005**, 3161–3165.
(43) Beissel, T.; Powers, R. E.; Parac, T. N.; Raymond, K. N. *J. Am. Chem. Soc.* **1999**, *121*, 4200–4206.
(44) Saalfrank, R. W.; Maid, H.; Scheurer, A.; Puchta, R.; Bauer, W. *Eur. J. Inorg. Chem.* **2010**, 2903–2906.
(45) Paul, R. L.; Argent, S. P.; Jeffery, J. C.; Harding, L. P.; Lynam, J. M.; Ward, M. D. *Dalton Trans.* **2004**, 3453–3458.
(46) Clayden, J.; Lund, A.; Vallverdu, L.; Helliwell, M. *Nature* **2004**, *431*, 966–971.
(47) Hennrich, G.; Anslyn, E. V. *Chem.—Eur. J.* **2002**, *8*, 2218–2224.
(48) Kelly, T. R.; Sestelo, J. P.; Tellitu, I. *J. Org. Chem.* **1998**, *63*, 3655–3665.
(49) Cohen, Y.; Avram, L.; Evan-Salem, T.; Frish, L. In *Analytical Methods in Supramolecular Chemistry*; Schalley, C., Ed.; Wiley-VCH: Weinheim, Germany: 2007; pp 163−219.
(50) Piguet, C.; Bernardinelli, G.; Hopfgartner, G. *Chem. Rev.* **1997**, *97*, 2005–2062.
(51) Albrecht, M. *Chem. Rev.* **2001**, *101*, 3457–3497.
(52) Glasson, C. R. K.; Meehan, G. V.; Clegg, J. K.; Lindoy, L. F.; Smith, J. A.; Keene, F. R.; Motti, C. *Chem.—Eur. J.* **2008**, *14*, 10535–10538.
(53) Li, F.; Clegg, J. K.; Lindoy, L. F.; MacQuart, R. B.; Meehan, G. V. *Nat. Commun.* **2011**, *2*, 205.
(54) Childs, L. J.; Alcock, N. W.; Hannon, M. J. *Angew. Chem., Int. Ed.* **2002**, *41*, 4244–4247.
(55) El-ghayouy, A.; Harriman, A.; Cian, A. D.; Fischer, J.; Ziessel, R. *J. Am. Chem. Soc.* **1998**, *120*, 9973–9974.
(56) *WINNMR*, version 950901.0; Bruker-Franzen Analytik GmbH.
(57) *CAChe*, version 7.5.0.85; Fujitsu Limited.
(58) Saalfrank, R. W.; Horner, B.; Stalke, D.; Salbeck, J. *Angew. Chem., Int. Ed.* **1993**, *32*, 1179–1182.
(59) Glasson, C. R. K.; Clegg, J. K.; McMurtrie, J. C.; Meehan, G. V.; Lindoy, L. F.; Motti, C. A.; Moubaraki, B.; Murray, K. S.; Cashion, J. D. *Chem. Sci.* **2011**, *2*, 540–543.
(60) Riddell, I. A.; Smulders, M. M. J.; Clegg, J. K.; Nitschke, J. R. *Chem. Commun.* **2011**, *47*, 457–459.
(61) Förster, H.; Vögtle, F. *Angew. Chem., Int. Ed. Engl.* **1977**, *16*, 429–441.
(62) Chaumeil, H.; Le Drian, C.; Defoin, A. *Synthesis* **2002**, 757–760.
(63) Kim, S.-H.; Tokarski, J. S.; Leavitt, K. J.; Fink, B. E.; Salvati, M. E.; Moquin, R.; Obermeier, M. T.; Trainor, G. L.; Vite, G. G.; Stadnick, L. K.; Lippy, J. S.; You, D.; Lorenzi, M. V.; Chen, P. *Bioorg. Med. Chem. Lett.* **2008**, *18*, 634–639.
(64) Kaur, I.; Jazdzyk, M.; Stein, N. N.; Prusevich, P.; Miller, G. P. *J. Am. Chem. Soc.* **2010**, *132*, 1261–1263.
(65) Han, Z.; Pinkner, J. S.; Ford, B.; Obermann, R.; Nolan, W.; Wildman, S. A.; Hobbs, D.; Ellenberger, T.; Cusumano, C. K.; Hultgren, S. J.; Janetka, J. W. *J. Med. Chem.* **2010**, *53*, 4779–4792.
(66) Ye, Y.-S.; Huang, Y.-J.; Cheng, C.-C.; Chang, F.-C. *Chem. Commun.* **2010**, *46*, 7554–7556.
(67) Davis, A. V.; Fiedler, D.; Ziegler, M.; Terpin, A.; Raymond, K. N. *J. Am. Chem. Soc.* **2007**, *129*, 15354–15363.
(68) Biros, S. M.; Yeh, R. M.; Raymond, K. N. *Angew. Chem., Int. Ed.* **2008**, *47*, 6062–6064.
(69) Clegg, J. K.; Li, F.; Jolliffe, K. A.; Meehan, G. V.; Lindoy, L. F. *Chem. Commun.* **2011**, *47*, 6042–6044.
(70) Scherer, M.; Caulder, D. L.; Johnson, D. W.; Raymond, K. N. *Angew. Chem., Int. Ed.* **1999**, *38*, 1588–1592.
(71) Corbett, P. T.; Leclaire, J.; Vial, L.; West, K. R.; Wietor, J. L.; Sanders, J. K. M.; Otto, S. *Chem. Rev.* **2006**, *106*, 3652–3711.
(72) Lehn, J. M.; Eliseev, A. V. *Science* **2001**, *291*, 2331–2332.
(73) Hutin, M.; Cramer, C. J.; Gagliardi, L.; Rehaman, A.; Bernardinelli, G.; Cerny, R.; Nitschke, J. R. *J. Am. Chem. Soc.* **2007**, *129*, 8774–8780.
(74) Fiedler, D.; Leung, D. H.; Bergman, R. G.; Raymond, K. N. *Acc. Chem. Res.* **2004**, *38*, 349–358.
(75) Hasegawa, T.; Furusho, Y.; Katagiri, H.; Yashima, E. *Angew. Chem., Int. Ed.* **2007**, *46*, 5885–5888.
(76) Kang, J.; Rebek, J. *Nature* **1997**, *385*, 50–52.
(77) Murase, T.; Horiuchi, S.; Fujita, M. *J. Am. Chem. Soc.* **2010**, *132*, 2866–2867.
(78) Annunziata, R.; Benaglia, M.; Cinquini, M.; Cozzi, F.; Woods, C. R.; Siegel, J. S. *Eur. J. Org. Chem.* **2001**, 173–180.
(79) Cantekin, S.; Balkenende, D. W. R.; Smulders, M. M. J.; Palmans, A. R. A.; Meijer, E. W. *Nat. Chem.* **2011**, *3*, 42–46.
(80) Wilson, A. J.; van Gestel, J.; Sijbesma, R. P.; Meijer, E. W. *Chem. Commun.* **2006**, 4404–4406.
(81) Woods, C. R.; Benaglia, M.; Cozzi, F.; Siegel, J. S. *Angew. Chem., Int. Ed.* **1996**, *35*, 1830–1833.
(82) Allen, F. *Acta Crystallogr.* **2002**, *B58*, 380–388.
(83) Lunazzi, L.; Mazzanti, A.; Minzoni, M.; Anderson, J. E. *Org. Lett.* **2005**, *7*, 1291–1294.
(84) Yamashita, K.-i.; Sato, K.-i.; Kawano, M.; Fujita, M. *New J. Chem.* **2009**, *33*, 264–270.
(85) Jones, P. G.; Zemanek, A.; Kus, P. *Acta Crystallogr.* **2007**, *C63*, o73–o76.
(86) Davies, N. R.; Dwyer, F. P. *Trans. Faraday Soc.* **1954**, *50*, 1325–1331.
(87) Seiden, L.; Basolo, F.; Neumann, H. M. *J. Am. Chem. Soc.* **1959**, *81*, 3809–3813.
(88) Bremer, S.; Trapp, O. *Electrophoresis* **2009**, *30*, 329–336.
(89) Tachiyashiki, S.; Yamatera, H. *Bull. Chem. Soc. Jpn.* **1981**, *54*, 3340–3346.
(90) Voshell, S. M.; Lee, S. J.; Gagne, M. R. *J. Am. Chem. Soc.* **2006**, *128*, 12422–12423.
(91) Ludlow, R. F.; Otto, S. *Chem. Soc. Rev.* **2008**, *37*, 101–108.
(92) Palmer, L. C.; Stupp, S. I. *Acc. Chem. Res.* **2008**, *41*, 1674–1684.
(93) Hernandez, J. V.; Kay, E. R.; Leigh, D. A. *Science* **2004**, *306*, 1532–1537.
(94) Eelkema, R.; Pollard, M. M.; Katsonis, N.; Vicario, J.; Broer, D. J.; Feringa, B. L. *J. Am. Chem. Soc.* **2006**, *128*, 14397–14407.
(95) Cram, D. J. *Nature* **1992**, *356*, 29–36.
(96) Hamilton, T. D.; MacGillivray, L. R. *Cryst. Growth Des.* **2004**, *4*, 419–430.
(97) Gottlieb, H. E.; Kotlyar, V.; Nudelman, A. *J. Org. Chem.* **1997**, *62*, 7512–7515.
(98) Hooft, R. W. W. *COLLECT*; Nonius B.V.: Delft, The Netherlands, 1998.
(99) Otwinowski, Z.; Minor, W. *Methods Enzymol.* **1997**, *276*, 307–326.
(100) Farrugia, L. *J. Appl. Crystallogr.* **1999**, *32*, 837–838.
(101) Altomare, A.; Burla, M. C.; Camalli, M.; Cascarano, G. L.; Giocavazzo, C.; Gaugliardi, A.; Moliterni, G. C.; Polidori, G.; Spagna, S. *J. Appl. Crystallogr.* **1999**, *32*, 115–119.
(102) Sheldrick, G. M. *SADABS*; University of Göttingen: Göttingen, Germany, 1996−2008.
(103) Sheldrick, G. M. *SHELXL-97*; University of Göttingen: Göttingen, Germany, 1997.
(104) Spek, A. L. *PLATON*; Utrecht University: Utrecht, The Netherlands, 2008.